182 *Organometallics* 1992, *11*, 182-191

Electronic and Steric Effects in Pentacoordinate Anionic Diorganotrifluorosilicates: X-ray Structures and ^{13}C NMR Studies for Evaluation of Charge Distribution in Aryl Groups on Silicon

Kohei Tamao,* Takashi Hayashi, and Yoshihiko Ito*

Department of Synthetic Chemistry, Faculty of Engineering, Kyoto University, Kyoto 606, Japan

Motoo Shiro

Shionogi Research Laboratory, Fukushima-ku, Osaka 553, Japan

Received July 25, 1991

A series of diorganotrifluorosilicates, $(4\text{-}XC_6H_4)MeSiF_3^-$ (1), $(4\text{-}XC_6H_4)PhSiF_3^-$ (2), $(Me_nC_6H_{5-n})PhSiF_3^-$ (3), $(2\text{-}MeC_6H_4)(4\text{-}MeC_6H_4)SiF_3^-$ (4), and $(2,6\text{-}Me_2C_6H_3)(3,5\text{-}Me_2C_6H_3)SiF_3^-$ (5) with the 18-crown-6 potassium countercation were prepared. Moleculr structures of **2a** ($X = CF_3$), **2d** ($X = Me$), **2e** ($X = MeO$), **2f** ($X = Me_2N$), **4**, and **5** were determined by X-ray crystallography, confirming trigonal-bipyramidal structures. The dihedral angle between the substituted phenyl group and the equatorial plane depends not on the electronic effect but on the steric effect. Variable-temperature ^{19}F NMR studies on **2** provide the electronic effects on energy barriers for pseudorotation. In ^{13}C NMR studies, all carbon chemical shifts have been observed and assigned unambiguously: the Si ipso carbons of aromatic rings and the methyl group have been observed for the first time. Changes in chemical shifts $\Delta\delta$(C) of anionic pentacoordinate silicates (**1** and **2**) vs the corresponding neutral tetracoordinate silanes (**6** and **7**) are +17 to +20 ppm for Si ipso (C1), +3 to +4 ppm for ortho (C2), −3 ppm for meta (C3), −4 to −7 ppm for para (C4), and +9 ppm for methyl carbon. The charge distribution in the phenyl groups in silicates has been discussed in terms of the electron-donating nature by the $-SiRF_3^-$ group via the π polarization effect. There are linear correlations of the chemical shifts of Si ipso C1 (para to X) in the para-substituted phenyl groups and Si ipso C1′ in the parent phenyl groups in **2** and **7** with the Hammett σ_p^+, from which are estimated the relative electron densities on Si ipso carbons C1 and C1′.

Introduction

It has been well recognized that penta- and hexacoordinate silicon species play an important role in reactions or organosilicon compounds.[1] Pentacoordinate anionic silicates have thus recently received much attention from structural and mechanistic points of view,[1] including structure determination,[2] nature of bonding,[3] intramolecular ligand exchange (Berry pseudorotation),[4] intermolecular ligand exchange with tetracoordinate silanes,[5] enhanced reactivity toward nucleophiles,[6] and activation of the silicon–carbon bonds toward electrophiles.[7]

While structural aspects from the steric viewpoints have so far been discussed extensively, mainly by the Holmes group,[2c,f,4c–e] studies on the electronic effect in pentacoordinate silicon species have been restricted mostly to the pseudorotation.[4a,e,f] Quite recently, a systematic, theoretical study on charge densities on silicon in tetra- and pentacoordinate silicon species has been reported by Deiter and Holmes;[3f] interestingly, their study has shown comparable charge densities in both cases.

We have been concerned with synthetic and mechanistic studies on cleavage reactions of silicon–carbon bonds, most of which have been believed to proceed through penta- and/or hexacoordinate silicon species.[7a–e] In connection with mechanistic studies, we now report herein the X-ray

---

[1] Review: (a) Tandura, St. N.; Alekseev, N. V.; Voronkov, M. G. *Top. Curr. Chem.* **1986**, *131*, 99–189. (b) Corriu, R. J. P.; Young, J. C. In *The Chemistry of Organic Silicon Compounds*; Patai, S., Rappoport, Z., Ed.; John Wiley: Chichester, England 1989; p 1241. (c) Holmes, R. R. *Chem. Rev.* **1990**, *90*, 17. (d) Corriu, R. J. P. *J. Organomet. Chem.* **1990**, *400*, 81.

[2] (a) Schomburg, D. *J. Organomet. Chem.* **1981**, *221*, 137. (b) Schomburg, D.; Krebs, R. *Inorg. Chem.* **1984**, *23*, 1378. (c) Harland, J. J.; Payne, J. S.; Day, R. O.; Holmes, R. R. *Inorg. Chem.* **1987**, *26*, 760. (d) Kira, M.; Sato, K.; Kabuto, C.; Sakurai, H. *J. Am. Chem. Soc.* **1989**, *111*, 3747. (e) Dixon, D. A.; Hertler, W. R.; Chase, D. B.; Farnham, E. B.; Davidson, F. *Inorg. Chem.* **1988**, *27*, 4012. (f) Kumara Swamy, K. C.; Chandrasekhar, V.; Harland, J. J.; Holmes, J. M.; Day, R. O.; Holmes, R. R. *J. Am. Chem. Soc.* **1990**, *112*, 2341.

[3] E.g.: (a) Damrauer, R.; Burggraf, L. W.; Davis, L. P.; Gordon, M. S. *J. Am. Chem. Soc.* **1988**, *110*, 6601. (b) Gronert, S.; Glaser, R.; Streitwieser, A. *J. Am. Chem. Soc.* **1989**, *111*, 3111. (c) Sini, G.; Ohanessian, G.; Hiberty, P. C.; Shaik, S. S. *J. Am. Chem. Soc.* **1990**, *112*, 1407. (d) Reed, A. E.; Schleyer, P. v. R. *J. Am. Chem. Soc.* **1990**, *112*, 1434. (e) Gordon, M. S.; Windus, T. L.; Burggraf, L. W.; Davis, L. P. *J. Am. Chem. Soc.* **1990**, *112*, 7167. (f) Deiter, J. A.; Holmes, R. R. *J. Am. Chem. Soc.* **1990**, *112*, 7197.

[4] Recent papers: (a) Stevenson, W. H., III; Wilson, S.; Martin, J. C.; Farnham, W. B. *J. Am. Chem. Soc.* **1985**, *107*, 6340. (b) Damrauer, R.; Danahey, S. E. *Organometallics* **1986**, *5*, 1490. (c) Johnson, S. E.; Day, R. O.; Holmes, R. R. *Inorg. Chem.* **1989**, *28*, 3182. (d) Johnson, S. E.; Payne, J. S.; Day, R. O.; Holmes, J. M.; Holmes, R. R. *Inorg. Chem.* **1989**, *28*, 3190. (e) Johnson, S. E.; Deiters, J. A.; Day, R. O.; Holmes, R. R. *J. Am. Chem. Soc.* **1989**, *111*, 3250. (f) Damrauer, R.; O'Connell, D.; Danahey, S. E.; Simon, R. *Organometallics* **1989**, *8*, 1167. (g) Tamao, K.; Hayashi, T.; Ito, Y.; Shiro, M. *J. Am. Chem. Soc.* **1990**, *112*, 2422.

[5] (a) Brownstein, S. *Can. J. Chem.* **1980**, *58*, 1407. (b) Marat, R. K.; Janzen, A. F. *Can. J. Chem.* **1977**, *55*, 1167 and 3845. (c) Klanberg, F.; Muetterties, E. L. *Inorg. Chem.* **1968**, *7*, 155.

[6] (a) Review: Corriu, R. J. P. *Pure Appl. Chem.* **1988**, *60*, 99. (b) Webster, O. W.; Hertler, W. R.; Sogah, D. Y.; Farnham, W. B.; RajanBabu, T. V. *J. Am. Chem. Soc.* **1983**, *105*, 5706. (c) Boudin, A.; Cerveau, G.; Chuit, C.; Corriu, R. J. P.; Reye, C. *Bull. Chem. Soc. Jpn.* **1988**, *101*, 61. (d) Boudin, A.; Cerveau, G.; Chuit, C.; Corriu, R. J. P.; Reye, C. *Organometallics* **1988**, *7*, 1165. (e) Chuit, C.; Corriu, R. J. P.; Reye, J. *Organomet. Chem.* **1988**, *358*, 57. (f) Hayashi, T.; Matsumoto, Y.; Kiyoi, T.; Ito, Y.; Kohra, S.; Tominaga, Y.; Hosomi, A. *Tetrahedron Lett.* **1988**, *29*, 5667. (g) Carre, F.; Cerveau, G.; Chuit, C.; Corriu, R. J. P.; Reye, C. *Angew. Chem., Int. Ed. Engl.* **1989**, *28*, 489 and references cited therein. (h) Sakurai, H. *Synlett* **1989**, 1. (i) Sato, K.; Kira, M.; Sakurai, H. *J. Am. Chem. Soc.* **1989**, *11*, 6429. (j) Kira, M.; Sato, K.; Sakurai, H. *J. Am. Chem. Soc.* **1990**, *112*, 257. (k) Chopra, S. K.; Martin, J. C. *J. Am. Chem. Soc.* **1990**, *112*, 5342.

[7] (a) Review: Kumada, M.; Tamao, K.; Yoshida, J. *J. Organomet. Chem.* **1982**, *239*, 115. (b) Tamao, K. In *Organosilicon and Bioorganosilicon Chemistry*; Sakurai, H., Ed.; Ellis Horwood: Chichester, England, 1985; pp 231–242. (c) Tamao, K.; Akita, M.; Maeda, K.; Kumada, M. *J. Org. Chem.* **1987**, *52*, 1100. (d) Tamao, K.; Akita, M.; Kato, H.; Kumada, M. *J. Organomet. Chem.* **1988**, *341*, 165. (e) Tamao, K. *J. Synth. Org. Chem., Jpn.* **1988**, *46*, 861. (f) Kuwajima, I.; Nakamura, E.; Hashimoto, K. *Tetrahedron* **1983**, *39*, 975. (g) Sheldon, J. C.; Hayes, R. N.; Bowie, J. H.; DePuy, C. H. *J. Chem. Soc., Perkin Trans. 2* **1987**, 275. (h) Yamamoto, Y.; Takeda, Y.; Akiba, K. *Tetrahedron Lett.* **1989**, *30*, 725. (i) Hatanaka, Y.; Hiyama, T. *J. Am. Chem. Soc.* **1990**, *112*, 7793.

0276-7333/92/2311-0182$03.00/0

Table I. Selected Bond Lengths (Å) and Angles (deg) for 2a, 2d–f, 4, and 5[a]

	2a	2d	2e	2f	4	5
			Distances			
Si–F1	1.677 (3)	1.673 (4)	1.683 (3)	1.679 (4)	1.701 (4)	1.687 (4)
Si–F2	1.639 (3)	1.678 (4)	1.636 (3)	1.636 (4)	1.636 (5)	1.621 (5)
Si–F3	1.717 (2)	1.722 (3)	1.713 (2)	1.721 (4)	1.713 (4)	1.723 (4)
Si–C1	1.918 (4)	1.901 (5)	1.898 (4)	1.899 (5)	1.904 (6)	1.899 (5)
Si–C7	1.893 (4)	1.899 (4)	1.903 (4)	1.909 (5)	1.889 (6)	1.908 (5)
K–F2	2.882 (3)	2.846 (3)	2.902 (3)	2.984 (4)	2.760 (5)	*b*
K–F3	2.661 (2)	2.653 (3)	2.622 (2)	2.596 (4)	2.731 (4)	2.512 (4)
			Angles			
F1–Si–F2	89.6 (1)	89.2 (2)	89.1 (1)	89.7 (2)	88.4 (2)	89.7 (2)
F1–Si–F3	175.0 (1)	174.8 (2)	175.7 (1)	175.7 (2)	175.9 (2)	176.0 (2)
F1–Si–C1	91.5 (1)	91.9 (2)	91.5 (1)	91.9 (2)	91.0 (2)	91.9 (2)
F1–Si–C7	91.8 (1)	91.5 (2)	91.4 (1)	91.2 (2)	90.6 (2)	90.4 (2)
F2–Si–F3	85.4 (1)	85.7 (2)	86.7 (1)	86.0 (2)	87.5 (2)	86.5 (2)
F2–Si–C1	119.7 (1)	119.8 (2)	118.6 (1)	119.6 (2)	117.4 (3)	117.5 (2)
F2–Si–C7	118.3 (1)	117.7 (2)	116.5 (2)	116.5 (2)	115.8 (3)	117.7 (2)
F3–Si–C1	90.8 (1)	90.9 (2)	90.6 (1)	90.8 (2)	91.0 (2)	91.0 (2)
F3–Si–C7	90.7 (1)	90.7 (2)	90.5 (2)	90.0 (2)	91.1 (2)	90.2 (2)
C1–Si–C7	121.9 (2)	122.4 (2)	124.9 (2)	123.8 (2)	126.8 (3)	124.8 (2)

[a] Estimated standard deviations in parentheses. The atom-labeling scheme is shown in Figure 1. [b] Longer than 3.5 Å.

structures and/or ^{19}F and ^{13}C NMR studies of phenylmethyl- and diphenyltrifluorosilicates with para or ortho substituents on the phenyl ring, in comparison with the corresponding tetracoordinate diorganodifluorosilanes, to clarify the electronic and steric perturbations in organic groups upon formation of anionic pentacoordinate silicon species. In particular, the observation of all carbons including the Si ipso carbon chemical shifts has made it possible for the first time to estimate the electron distribution in the phenyl rings and the charge densities of the Si ipso carbons which should govern the reactivity of the silicon–carbon bonds.

Results and Discussion

Synthesis. A series of diorganotrifluorosilicates, $(4\text{-}XC_6H_4)MeSiF_3^-$ (**1**), $(4\text{-}XC_6H_4)PhSiF_3^-$ (**2**), $(Me_nC_6H_{5-n})PhSiF_3^-$ (**3**), $(2\text{-}MeC_6H_4)(4\text{-}MeC_6H_4)SiF_3^-$ (**4**), and $(2,6\text{-}Me_2C_6H_3)(3,5\text{-}Me_2C_6H_3)SiF_3^-$ (**5**), with the 18-crown-6 potassium countercation were examined in this study. These were prepared by Damrauer's elegant method[4b] from the corresponding difluorosilanes by treatment with spray-dried KF in toluene in the presence of 18-crown-6 (eq 1) and purified by recrystallization from THF. The

$$R^1R^2SiF_2 + KF \xrightarrow[\text{toluene}]{\text{18-crown-6}} [R^1R^2SiF_3]^{(-)}\ K^{(+)}\cdot\text{18-crown-6} \qquad (1)$$

use of exactly 1 equiv or less of KF was essential for purification of the silicates by recrystallization: an excess amount of KF caused contamination with KF·18-crown-6 crystals.

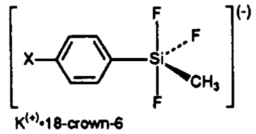

1
a: X = CF₃
b: X = Cl
c: X = H
d: X = Me
e: X = OMe

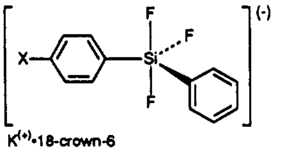

2
a: X = CF₃
b: X = Cl
c: X = H
d: X = Me
e: X = OMe
f: X = NMe₂

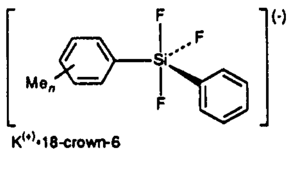

3
a: 2-Me
b: 3-Me
c: 2,6-Me₂
d: 3,5-Me₂
e: 2,4,6-Me₃

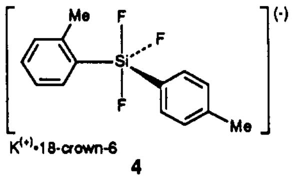

4

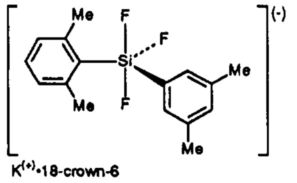

5

X-ray Crystal Structure. Molecular structures of $[(4\text{-}CF_3C_6H_4)PhSiF_3^-][K^+\cdot\text{18-crown-6}]$ (**2a**), $[(4\text{-}MeC_6H_4)PhSiF_3^-][K^+\cdot\text{18-crown-6}]$ (**2d**), $[(4\text{-}MeOC_6H_4)PhSiF_3^-][K^+\cdot\text{18-crown-6}]$ (**2e**), $[(4\text{-}Me_2NC_6H_4)PhSiF_3^-][K^+\cdot\text{18-crown-6}]$ (**2f**), $[(2\text{-}MeC_6H_4)(4\text{-}MeC_6H_4)SiF_3^-][K^+\cdot\text{18-crown-6}]$ (**4**), and $[(2,6\text{-}Me_2C_6H_3)(3,5\text{-}Me_2C_6H_3)SiF_3^-][K^+\cdot\text{18-crown-6}]$ (**5**) were determined by X-ray crystallography. The structures and the atom-labeling schemes are given in Figure 1. These represent the first determination of molecular structures of unsymmetrical diaryltrifluorosilicates.

Selected bond lengths and angles are given in Table I. All crystal data are summarized in Table II. Atomic coordinates, thermal parameters, and full data of bond lengths and angles are provided as supplementary material. Since the crystal of compound **4** was not good enough for refinement (R = 0.082, R_w = 0.126), the data will be omitted from the detailed discussions which follow.

Structural features are discussed on the basis of the representative data, listed in Table III, which contains bond lengths, bond angles, deviations of the Si atom out of the equatorial plane, deformation parameter (Δ),[2c] dihedral angles between the equatorial plane and aromatic rings, and the corresponding literature data of some related compounds for comparison.

(1) The molecular geometry about the silicon atom in **2** and **5** is referred to as trigonal bipyramidal (TBP) with two aryl groups in the equatorial positions. The bond lengths, bond angles, deviations of Si from the equatorial plane, and deformation parameter (Δ) are all not largely different from those of the parent counterpart, $Ph_2SiF_3^-$.[2b] Only the Si–C1 ($Si\text{–}C_6H_4CF_3$) bond in **2a**, 1.918 (4) Å, seems to be somewhat longer than other Si–C bonds in the diorganotrifluorosilicate series and comparable to Si–C bonds in a triaryldifluorosilicate, $1\text{-}NpPh_2SiF_2^-$.[2c]

(2) The potassium cation interacts with two fluorine atoms, one axial and one equatorial, with a shorter distance to the former. Of two axial Si–F bonds, the Si–F3 bond

Table II. Summary of Crystal Data, Intensity Collection, and Least-Squares Processing for 2a, 2d–f, 4 and 5

	2a	2d	2e	2f	4	5
formula	$C_{25}H_{33}O_6F_6SiK$	$C_{25}H_{36}O_6F_3SiK$	$C_{25}H_{36}O_7F_3SiK$	$C_{26}H_{39}NO_6F_3SiK$	$C_{26}H_{38}O_6F_3SiK$	$C_{28}H_{42}O_6F_3SiK$
fw	610.7	556.7	572.7	585.8	570.8	598.8
cryst sys	monoclinic	monoclinic	monoclinic	monoclinic	monoclinic	orthorhombic
space group	$P2_1/c$	$P2_1/c$	$P2_1/c$	$P2_1/c$	$P2_1/c$	$P2_12_12_1$
a, Å	8.259 (2)	8.381 (1)	8.297 (3)	8.455 (2)	8.523 (1)	17.872 (4)
b, Å	21.713 (2)	21.244 (1)	21.515 (3)	21.665 (4)	17.937 (2)	20.331 (5)
c, Å	17.623 (2)	17.399 (1)	17.604 (3)	17.416 (2)	20.347 (2)	8.553 (2)
β, deg	110.75 (1)	111.38 (1)	111.61 (2)	110.67 (1)	107.93 (1)	
V, Å^3	2955.2 (8)	2884.8 (5)	2922 (1)	2985.1 (9)	2959.5 (6)	3108 (1)
Z	4	4	4	4	4	4
$\rho calcd$, g cm^{-3}	1.373	1.282	1.302	1.303	1.281	1.280
μ(Cu Kα), cm^{-1}	26.2	24.7	24.8	24.2	24.2	23.3
$2\theta max$, deg	120	120	120	110	110	130
no. of unique reflns	4393	4288	4339	3644	3702	3000
no. of reflns, used for refinement	3694	3456	3465	2839	2809	2680
R	0.056	0.060	0.051	0.057	0.082	0.041
R_w	0.085	0.092	0.074	0.084	0.126	0.056
S	1.328	1.392	1.250	1.287	1.476	1.464

Table III. Comparison of Bond Lengths, Bond Angles, Deviations from Trigonal-Bipyramidal Geometry, and Dihedral Angles for Diaryltrifluorosilicates and Some Related Compounds[a]

	X in $(4\text{-}XC_6H_4)PhSiF_3^-$									
	CF_3 (2a)	Me (2d)	MeO (2e)	Me_2N (2f)	5	$Ph_2SiF_3^-$[b]	$Mes_2SiF_3^-$	$t\text{-}BuPhSiF_3^-$	1-$NpPh_2$-SiF_2^-[c]	$PhSiF_4^-$[b]
Si–F1$_{ax}$, Å	1.677 (3)	1.673 (4)	1.683 (3)	1.679 (4)	1.687 (4)	1.688	1.678 (6)	1.682 (4)	1.720 (4)	1.668
Si–F3$_{ax}$, Å[d]	1.713 (2)	1.722 (3)	1.713 (2)	1.721 (4)	1.723 (4)	1.688	1.729 (6)	1.718 (4)	1.720 (4)	1.670
Si–F2$_{eq}$, Å	1.639 (3)	1.638 (4)	1.636 (3)	1.636 (4)	1.621 (5)	1.648	1.641 (6)	1.639 (4)		1.601[e]
Si–C1$_{eq}$, Å	1.918 (4)	1.901 (5)	1.898 (4)	1.899 (5)	1.899 (5)	1.893	1.872 (9)	1.897 (6)[f]	1.925 (7)[g]	1.871
Si–C7$_{eq}$, Å	1.893 (4)	1.899 (4)	1.903 (4)	1.909 (5)	1.908 (5)	1.893	1.915 (7)	1.902 (6)	1.915 (7)	
deviation of Si from eq plane, Å	0.032 (1)	0.027 (2)	0.022 (1)	0.031 (2)	0.022 (2)		0.019	0.014		
F$_{ax}$–Si–F$_{ax}$, deg	175.0 (1)	174.8 (2)	175.7 (1)	175.7 (2)	176.0 (2)	198.6	175.6 (3)	171.9 (2)	176.4 (2)	174.6
C$_{eq}$–Si–C$_{eq}$, deg	121.9 (2)	122.4 (2)	124.9 (2)	123.7 (2)	124.8 (2)	118.9	127.0 (4)	124.3 (2)[h]	125.8 (3)	121.4[i]
Δ, deg[j]	6.9	7.6	9.2	8.1	8.9	8.7	11.4	12.4	9.4	6.8
dihedral angle, deg[k]										
C1–C6	86.1 (1)	83.5 (2)	74.1 (1)	87.9 (2)	65.9 (2)[l]	75	36.6	87	87.2	54.3
C7–C12	69.8 (1)	72.1 (2)	73.5 (1)	75.3 (2)	28.6 (2)[m]	75	32.8		58.4 34.8[n]	
ref	this work	this work	this work	this work	this work	2b	4e	4d	2c	2a

[a] Atom-labeling systems are shown in Figure 1. Unless otherwise stated, the countercation is K^+·18-crown-6. [b] Countercation is Me_4N^+. [c] 1-Np = 1-naphthyl. [d] Fluorine close to the countercation. [e] Average. [f] Si–t-Bu bond. [g] Si–Np bond. [h] F$_{eq}$–Si–C$_{eq}$. [i] F$_{eq}$–Si–F$_{eq}$. [j] The sum of axial and equatorial bond angle displacements from the values of 180 and 120°, respectively, for the ideal TBP structure (ref 2c). [k] Dihedral angle between the aryl group and equatorial plane. [l] 3,5-Xylyl group. [m] 2,6-Xylyl group. [n] Naphthyl group.

close to the K^+ ion is longer than the other in all cases.

(3) There are unusually large dihedral angles between the aryl ring and equatorial plane in some cases. Thus, the angle between the XC_6H_4 ring and equatorial plane in **2a**, **2d**, and **2f** is 86.1, 83.5, and 87.9°, respectively, being much larger than 75° or less which is found for the corresponding angles between the parent phenyl ring and equatorial plane in our series **2** and in $Ph_2SiF_3^-$ [2b] and $PhSiF_4^-$.[2a] There seems to be a tendency that equatorial aryl groups in the TBP structure inherently avoid being perpendicular to the equatorial plane because of steric repulsion between the ortho hydrogens and axial fluorines, as is seen in $Ph_2SiF_3^-$ and $PhSiF_4^-$. It is therefore of particular interest to note that the $Me_2NC_6H_4$ group in **2f** is almost perpendicular to the equatorial plane; the dihedral angle 87.9° is the largest ever reported for pentacoordinate silicates. The largest values, 87–87.2°, so far reported in literature have been found in $t\text{-}BuPhSiF_3^-$ [4d] and $1\text{-}NpPh_2SiF_2^-$,[2c] in which the phenyl group appears to be forced nearly perpendicular to the equatorial plane by the other bulky equatorial group. In our cases, in contrast, the electronic effect must be the primary factor, but since both the electron-withdrawing (CF_3) and electron-releasing (Me_2N) groups cause the perpendicular arrangement, the exact nature of the electronic effect would not readily be clarified.

The other extreme case has been observed in **5**. Thus, the 2,6-xylyl group rotates only 28.6° out of the equatorial plane, which is among the smallest angles. This is obviously owing to the steric hindrance by ortho substituents, as reported by Holmes and his co-workers: The smallest values for monoorgano- and diorganofluorosilicates were 13.8° in $(2,4,6\text{-}(t\text{-}Bu)_3C_6H_2)SiF_4^-$ [4c] and 30° in $(2\text{-}MeC_6H_4)_2SiF_3^-$.[4e]

(4) Another interesting structural feature is the extent of planarity of the dimethylamino group in **2f**; N1 deviates 0.169 (5) Å from the C4–C13–C14 plane. It has been known that the N–C(aromatic) bond length is well correlated with the planarity of the nitrogen atom based on the angle (ϕ) between the N–C(aromatic) and the bisector of the Me–N–Me moiety.[8] Thus, an electron-withdrawing group on the aromatic ring causes the coplanarity of amino group and the bond-shortening, as shown by some pertinent data listed in Table IV. The data reveal that the $-SiPhF_3^-$ group is a mild electron-releasing group, being in line with the result deduced from the ^{13}C NMR data (vide infra).

^{19}F NMR Study for Intramolecular Ligand Exchange. Like other known anionic pentacoordinate silicates,[4] diorganotrifluorosilicates prepared in this study all

---

(8) (a) Christen, D.; Norbury, D.; Lister, D. G.; Palmieri, P. *J. Chem. Soc., Faraday Trans. 2*, **1975**, *71*, 438. (b) Ohms, R.; Guth, H. *Z. Kristallogr.* **1984**, *166*, 213. (c) Nakai, H.; Saito, T.; Yamakawa, *Acta Crystallogr.* **1988**, *C44*, 533. (d) Nakai, H.; Saito, T.; Yamakawa, *Acta Crystallogr.* **1988**, *C44*, 1057.

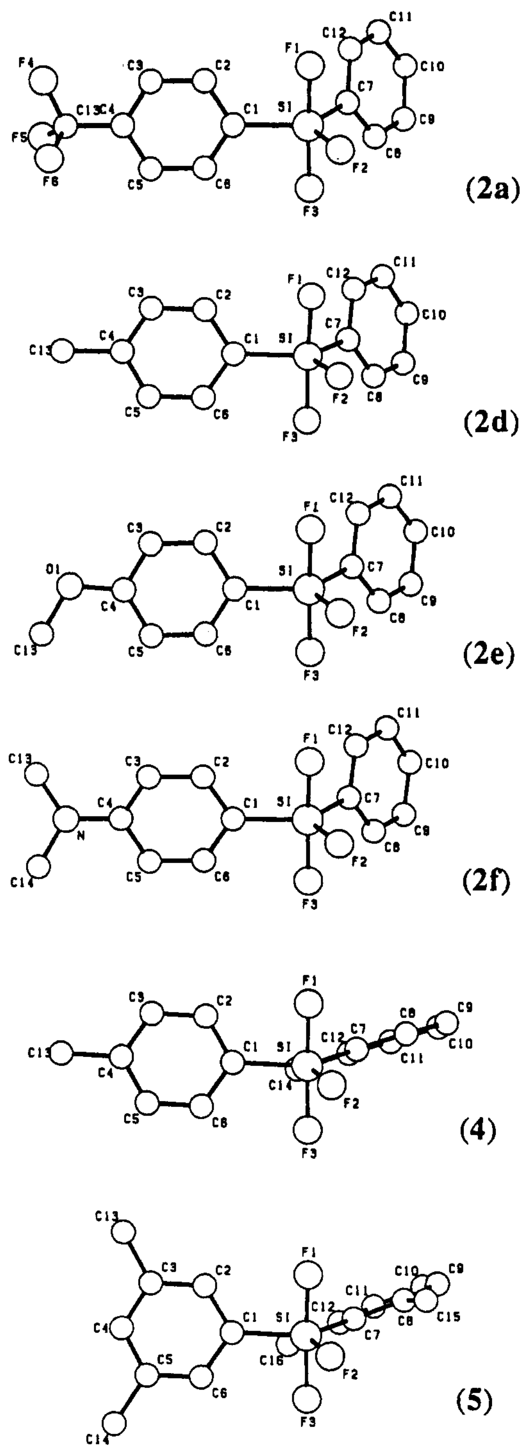

Figure 1. X-ray crystal structures of $[(4\text{-}CF_3C_6H_4)PhSiF_3^-][K^+\cdot18\text{-crown-6}]$ (**2a**), $[(4\text{-}MeC_6H_4)PhSiF_3^-][K^+\cdot18\text{-crown-6}]$ (**2d**), $[(4\text{-}MeOC_6H_4)PhSiF_3^-][K^+\cdot18\text{-crown-6}]$ (**2e**), $[(4\text{-}Me_2NC_6H_4)PhSiF_3^-][K^+\cdot18\text{-crown-6}]$ (**2f**), $[(2\text{-}MeC_6H_4)(4\text{-}MeC_6H_4)SiF_3^-][K^+\cdot18\text{-crown-6}]$ (**4**), and $[(2,6\text{-}Me_2C_6H_3)(3,5\text{-}Me_2C_6H_3)SiF_3^-][K^+\cdot18\text{-crown-6}]$ (**5**). The $K^+\cdot18$-crown-6 part is omitted from each structure for clarity.

undergo rapid ligand exchange via the Berry pseudorotation to show a singlet in the ^{19}F NMR spectrum at ambient temperatures, which, upon cooling to −78 °C, separates into two signals due to the apical and equatorial fluorine atoms. The data are given in the Experimental Section.

Table IV. Comparison of Coplanarity of the Dimethylamino Group and Bond Length in Dimethylamino/Aromatic Compounds

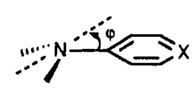

compd	φ, deg	N–C(aromatic), Å	ref
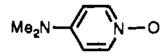	0.3	1.351	8c
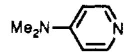	5.5	1.367	8b
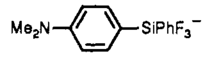 (2f)	20.0	1.402	this work
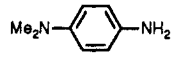	41.7 42.2	1.425 1.430	8d

Table V. Energy Barriers for Intramolecular Ligand Exchange of $[ArAr'SiF_3^-][K^+\bullet18\text{-crown-6}]$

silicate	$\Delta G^\ddagger$, kcal/mol	silicate	$\Delta G^\ddagger$, kcal/mol
2a	9.7	**2e**	10.8
2b	10.2	**3c**	11.6
2c	10.4	**5**	12.3

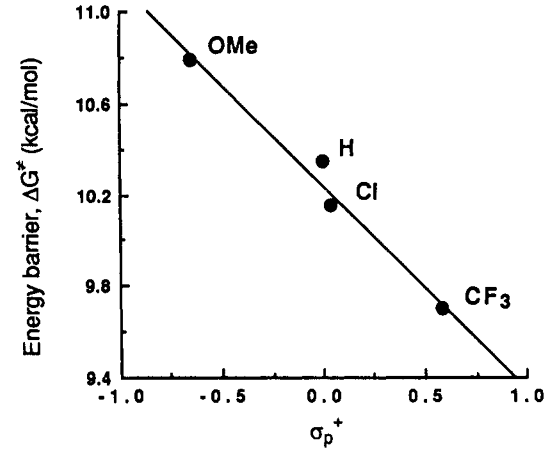

Figure 2. Hammett plot of energy barrier of the intramolecular ligand exchange of **2a**, **2b**, **2c**, and **2e**.

Variable-temperature ^{19}F NMR studies have been carried out on a series of $(4\text{-}XC_6H_4)PhSiF_3^-$ (**2**) for the purpose of elucidation of the electronic effects on the pseudorotation. The coalescence temperatures were around −10 to −20 °C. The energy barriers for the exchange are summarized in Table V. Thus, electron-withdrawing substituents facilitate the pseudorotation, being consistent with the previous results.[4a,f] A good linear relationship has been obtained between the energy barriers and the Hammett σ_p^+,[9] as shown in Figure 2, the ρ value being +2.0 (r = 0.977). Energy barriers for isomerization of 2,6-xylyl derivatives **3c** and **5** were also determined to be ca. 12 kcal/mol, as listed in Table V. The pseudorotation is clearly retarded by bulky groups, in consonant with Holmes'[4e] and Dramrauer's results.[4f]

^{13}C NMR Spectra. (A) Assignments. ^{13}C NMR spectra of silicates **1**–**5** were measured in acetone-d_6. All ring carbons were assigned unambiguously by the coupling pattern with fluorine atoms on silicon, relative intensities of signals, and/or the two-dimensional H–C COSY spectra. As typical examples, ^{13}C NMR spectra of pentacoordinate silicate **2c** and its tetracoordinate precursor **7c** are reproduced in Figure 3. The ^{13}C NMR data, chemical shifts, and coupling constants (J_{CF}) of silicates **1**–**5** and of the precursors **6** and **7** are summarized in Tables VI and VII. Several points deserve comment.

---

(9) Swain, C. G.; Lupton, E. C. *J. Am. Chem. Soc.* **1968**, *90*, 4328.

Table VI. ^{13}C NMR Data of Arylmethyltrifluorosilicates 1 at −78 °C and Arylmethyldifluorosilanes 6 at +22 °C[a]

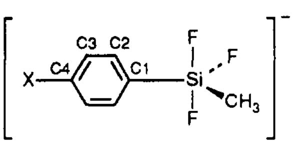

1

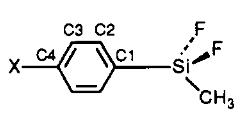

6

1 (X)[b]	C4	C3	C2 (t, $^3J_{CCSiF_{ap}}$)	C1 (dt, $^2J_{CSiF_{ap}}$ and $^2J_{CSiF_{eq}}$)	SiCH$_3$ (dt, $^2J_{CSiF_{ap}}$ and $^2J_{CSiF_{eq}}$)
1a (CF$_3$)[c]	128.50[d]	123.10[e]	138.29[e]	153.75[f]	3.85 (49.70 and 10.20)
1b (Cl)	133.32	126.71	140.31 (7.88)	146.38 (43.78 and 12.58)	4.12 (49.88 and 10.42)
1c (H)	127.89	126.77	138.34 (7.65)	147.59 (42.99 and 11.08)	4.31 (50.28 and 10.47)
1d (Me)[g]	136.88	127.57	138.74 (7.65)	143.67 (43.13 and 11.33)	4.43 (49.41 and 13.13)
1e (OMe)[h]	159.74	111.99	140.30 (7.80)	137.80 (42.63 and 11.37)	4.48 (50.95 and 10.08)

6 (X)	C4	C3	C2	C1 (t, $^2J_{CSiF}$)	SiCH$_3$ (t, $^2J_{CSiF}$)
6a (CF$_3$)[i]	133.91[j]	125.73[k]	135.19[l]	135.55 (19.25)	−5.13 (16.35)
6b (Cl)	138.82	129.42	136.05	129.19 (19.90)	−5.05 (16.83)
6c (H)	132.85	129.25	134.29	130.62 (19.18)	−5.03 (17.00)
6d (Me)[m]	143.14	129.94	134.35	127.12 (19.30)	−4.96 (17.20)
6e (OMe)[n]	163.62	114.95	136.10	121.43 (19.80)	−4.90 (17.48)

[a] Measured in acetone-d_6 at 50.29 MHz. Unless otherwise state, each signal appears as a singlet. Chemical shifts are recorded in δ ppm downfield, from TMS and coupling constants, in hertz. [b] 18-Crown-6 carbons appear at δ 70.21–70.27 (s). [c] CF$_3$ δ 125.52 (q, $^1J_{CF}$ = 269.58). [d] Quartet, $^2J_{CF}$ = 38.75. [e] Broad singlet. [f] Not measurable. [g] Me δ 21.15. [h] MeO δ 54.46. [i] CF$_3$ δ 124.92 (q, $^1J_{CF}$ = 270.13). [j] Quartet, $^2J_{CF}$ = 32.05. [k] Quartet, $^3J_{CF}$ = 3.75. [l] Quartet, $^4J_{CF}$ = 1.90. [m] Me δ 21.63. [n] OMe δ 55.47.

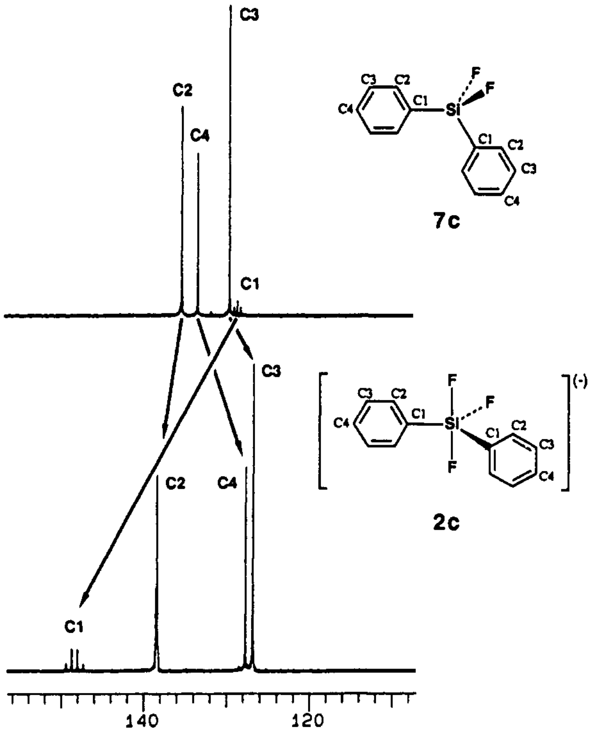

Figure 3. ^{13}C NMR spectra of Ph$_2$SiF$_2$ (7c) and [Ph$_2$SiF$_3^-$][K$^+$·18-crown-6] (2c) (aromatic region), recorded in acetone-d_6 at +20 °C.

This is the first case where the Si ipso carbons in anionic organofluorosilicates were observed successfully.[10,11] While the Si ipso carbons in diarylsilicates **2–5** could be observed at ambient temperatures, those in arylmethylsilicates **1** were observed only at low temperatures around −78 °C. Since the TBP structure of **1** is kept at low temperatures on the NMR time scale, the Si ipso carbons (C1) and the methyl carbons appear as double triplets having two different coupling constants $^2J_{CSiF_{ap}}$ (43–50 Hz) and $^2J_{CSiF_{eq}}$ (10–13 Hz) (Table VI). The Si ipso carbons (C1 and C1′) in **2–5** at ambient temperatures appear as quartets due to coupling with three equivalent fluorine atoms arising from rapid intramolecular exchange (Table VII). The coupling constants $^2J_{CSiF}$ (about 35 Hz) of the latter in the temperature range of rapid exchange are roughly equal to the average of two $^2J_{CSiF_{ap}}$ (43 Hz) and one $^2J_{CSiF_{eq}}$ (12 Hz) in the former. It may be further noted that the coupling constants $^2J_{CSiF}$ in pentacoordinate silicates **1–5** are nearly 1.5 times larger than those in tetracoordinate silanes **6** and **7**, although the origin is not clear at present.

There is an interesting tendency also in coupling between ortho carbons and fluorine atoms, $^3J_{CCSiF}$. Thus, ortho carbons (C2) of para-substituted phenyl groups in **1** existing as a "frozen" TBP structure at −78 °C appear as triplets due to coupling with two apical fluorines, having coupling constants $^3J_{CCSiF_{ap}}$ of ca. 8 Hz. In **2–5**, at +20 °C where these undergo rapid intramolecular ligand exchange, ortho carbons of the parent phenyl group and para- and meta-substituted phenyl groups appear as a quartet due to coupling with three equivalent fluorines, having coupling constants $^3J_{CCSiF}$ of ca. 5 Hz, nearly equal to two-thirds of the coupling constant in **1**. On the other hand, ortho carbons of ortho-substituted phenyl groups appear as singlets, as observed in **3a**, **3c**, **3e**, **4**, and **5**. This striking difference strongly suggests that the coupling is not through bonds, but by through-space attractions or through ortho hydrogen atoms, because such a coupling may be hindered by the ortho substituents in ortho-substituted phenyl groups.

(B) Charge Distribution in Aryl Groups in Silicates. ^{13}C chemical shift should afford useful information about the electronic nature of the particular carbon center.[13] In particular, the chemical shifts of carbon para to the substituent in monosubstituted benzenes have been

---

[10] ^{13}C NMR of tetracoordinate phenylsilane derivatives have been extensively studied: (a) Nguyen-Duc-Chuy, Chvalovsky, V.; Schraml, J.; Mage, M.; Lippmaa, E. *Coll. Czech. Chem. Commun.* **1975**, *40*, 875. (b) Schraml, J.; Chvalovsky, V.; Magi, M.; Lippmaa, E. *Coll. Czech. Chem. Commun.* **1975**, *40*, 897. (c) Rakita, P. E.; Worsham, L. S. *J. Organomet. Chem.* **1977**, *137*, 145.

[11] ^{13}C NMR data of pentacoordinate aryl–silicon compounds are available for only a few compounds such as silatranes and analogues,[1a,12] and anionic phenylsilicates.[4b,4f] Si ipso carbons in pentacoordinate arylfluorosilicates have never been reported so far.

[12] Harris, R. K.; Jones, J.; Ng, S. *J. Magn. Reson.* **1978**, *30*, 521.

[13] A linear relationship of δ(C$_{para}$) with the total charge densities (factor 450 ppm/e): (a) Hehre, W. J.; Taft, R. W.; Topsom, R. D. *Prog. Phys. Org. Chem.* **1976**, *12*, 159. (b) Hansen, P. E. *Org. Magn. Reson.* **1979**, *12*, 109.

Table VII. ^{13}C **NMR Data of Diaryltrifluorosilicates 2–5 and Diaryldifluorosilanes 7 at +22 °C**[a]

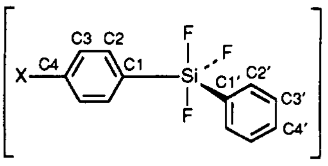

2

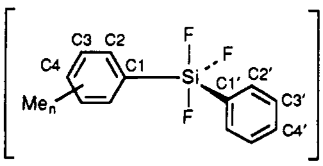

3

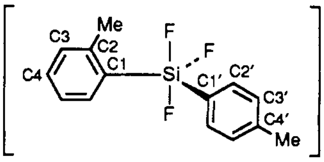

4

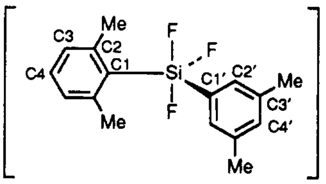

5

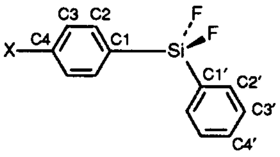

7

	XC_6H_4				C_6H_5			
2 (X)[b]	C4	C3	C2 (q, $^3J_{CCSiF}$)	C1 (q, $^2J_{CSiF}$)	C4′	C3′	C2′ (q, $^3J_{CSiF}$)	C1′ (q, $^2J_{CSiF}$)
2a (CF_3)[c]	128.96[d]	123.16[e]	138.64 (4.75)	154.94 (35.60)	128.06	126.99	138.43 (4.65)	147.55 (33.20)
2b (Cl)	133.45	126.89	140.33 (4.95)	148.02 (34.88)	127.86	126.79	138.49 (4.72)	147.54 (35.95)
2c (H)	127.71	126.84	138.41 (4.75)	148.40 (34.88)	127.71	126.84	138.41 (4.75)	148.40 (34.88)
2d (Me)[f]	136.70	127.66	138.90 (4.85)	144.88 (34.60)	127.54	126.77	138.40 (4.62)	149.02 (35.10)
2e (OMe)[g]	160.34	112.45	140.45 (5.15)	139.21 (34.80)	127.47	126.74	138.31 (4.53)	149.18 (35.00)
	substituted phenyl				phenyl			
3[b]	C4	C3	C2 (q, $^3J_{CCSiF}$)	C1 (q, $^2J_{CSiF}$)	C4′	C3′	C2′ (q, $^3J_{CSiF}$)	C1′ (q, $^2J_{CSiF}$)
3a (2-Me)[h]	128.04[i]	126.11 123.83	141.26[j] 134.25	149.74 (37.50)	128.85[i]	126.94	139.15 (4.65)	147.64 (32.83)
3b (3-Me)[k]	126.84[i]	135.21[j] 128.32[i]	139.13 (4.42) 135.46 (4.48)	148.54 (34.57)	127.69[i]	126.84[i]	138.43 (4.67)	148.54 (34.92)
3c (2,6-Me_2)[l]	127.85[i]	125.75[i]	141.14[j]	149.30 (38.82)	127.03[i]	126.81[i]	138.93 (5.15)	149.83 (32.50)
3d (3,5-Me_2)[m]	127.66[i]	135.10[j]	136.20 (4.23)	148.66 (35.02)	129.22[i]	126.82	138.46 (4.45)	148.08 (34.30)
3e (2,4,6-Me_3)[n]	134.21[j]	127.71	141.32[j]	145.76 (38.82)	127.71	126.99	138.95 (5.05)	150.05 (32.53)
	2-MeC_6H_4				4′-MeC_6H_4			
4[b],[o]	C4	C3	C2 (q, $^3J_{CCSiF}$)	C1 (q, $^2J_{CSiF}$)	C4′	C3′	C2′ (q, $^3J_{CSiF}$)	C1′ (q, $^2JC_{SiF}$)
	128.80[i]	126.04[i] 123.79[i]	141.20[j] 134.22	149.89 (36.87)	137.12[j]	127.80[i]	139.44 (4.20)	143.79 (32.58)
	2,6-$Me_2C_6H_3$				3,5-$Me_2C_6H_3$			
5[b,p]	C4	C3	C2 (q, $^3J_{CCSiF}$)	C1 (q, $^2J_{CSiF}$)	C4′	C3′	C2′ (q, $^3J_{CSiF}$)	C1′ (q, $^2J_{CSiF}$)
	129.37[i]	126.80	141.28[j]	149.40 (38.10)	125.74[i]	135.25[j]	136.58 (4.77)	149.57 (32.03)
7 (X)[b]	C4	C3	C2	C1 (t, $^2J_{CSiF}$)	C4′	C3′	C2′	C1′ (t,$2J_{CSiF}$)
7a (CF_3)[q]	134.24[r]	125.95[s]	136.06	135.80[t]	133.64	129.58	135.21	127.50 (19.45)
7b (Cl)	139.29	129.65	136.89	127.87 (22.30)	133.41	129.45	135.08	127.13 (20.45)
7c (H)	133.24	129.40	135.11	128.49 (19.90)	133.24	129.40	135.11	128.49 (19.90)
7d (Me)[u]	143.67	130.13	135.20	124.94 (20.13)	133.16	129.37	135.11	128.80 (20.15)
73 (Ome)[v]	163.92	115.16	137.02	119.10 (20.53)	133.06	129.33	135.10	129.00 (22.49)

[a] Measured in acetone-d_6 at 50.29 MHz. Unless otherwise stated, each signal appears as a singlet. Chemical shifts are recorded in δ ppm downfield from TMS, and coupling constants, in hertz. [b] 18-Crown-6 carbons appear at δ 70.57–70.83 (s). [c] CF_3 δ 126.06 (q, $^1J_{CF} = 269.95$). [d] Quartet, $^2J_{CF} = 30.65$. [e] Quartet, $^3J_{CF} = 3.65$. [f] Me δ 21.35. [g] MeO δ 54.89. [h] Me δ 23.78. [i] Tentative assignments. [j] Me-substituted carbon. [k] Me δ 21.78. [l] Me δ 24.64. [m] Me δ 21.67. [n] 2,6-Me_2 δ 24.52; 4-Me δ 21.02. [o] 2-Me δ 23.78; 4-Me δ 21.35. [p] 2,6-Me_2 δ 23.56; 3,5-Me_2 δ 21.19. [q] CF_3 δ 124.88 (q, $^1J_{CF} = 270.15$). [r] Quartet, $^2J_{CF} = 32.05$. [s] Quartet, $^3J_{CF} = 3.77$. [t] Indistinguishable. [u] Me δ 21.68. [v] OMe δ 55.52.

well correlated with the total charge density of the para carbon.[13,14]

(1) The electronic effects on the benzene ring exerted by $-SiPhF_2$ and $-SiPhF_3^-$ groups as nuclear substituents are discussed first. Differences in chemical shifts of all carbons in Ph_2SiF_2 (**7c**) and $Ph_2SiF_3^-$ (**2c**) from that of benzene (δ 129.1 ppm in acetone-d_6), $\Delta\delta(C(\mathbf{7c} - C_6H_6))$ and $\Delta\delta(C(\mathbf{2c} - C_6H_6))$, are shown in **A** and **B**, respectively, in Figure 4. Throughout this paper, a positive sign means a downfield shift. In the tetracoordinate case **7c**, C2 and C4 show small downfield shifts relative to those of benzene, keeping C1 and C3 almost unperturbed, while in the case of pentacoordinate **2c**, C1 and C2 show downfield shifts and C3 and C4 small upfield shifts. Comparison of these C4 chemical shifts indicates a weak electron-accepting nature of the $-SiPhF_2$ group, as reported previously,[9] and an electron-releasing nature of the $-SiPhF_3^-$ group.[15]

For evaluation of the electronic effect of the $-SiPhF_3^-$ group, we next discuss the chemical shift changes upon formation of pentacoordinate anionic silicates, **2c** and **1c**, from tetracoordinate neutral silanes, **7c** and **6c**, respectively; the data, $\Delta\delta(C(\mathbf{2c} - \mathbf{7c}))$ and $\Delta\delta(C(\mathbf{1c} - \mathbf{6c}))$, are

---

[14] A linear relationship of $\delta(C_{para})$ with σ^+ and with the total charge densities (factor 286 ppm/charge unit): Nelson, G. L.; Levy, G. C.; Cargioli, J. D. *J. Am. Chem. Soc.* **1972**, *94*, 3089.

[15] Substituent constants for σ inductive and resonance effects may be estimated to be $\sigma_I = +0.53$ and $\sigma_R{}^\circ = +0.19$ for the $-SiPhF_2$ group and $\sigma_I = -1.02$ and $\sigma_R{}^\circ = +0.04$ for the $-SiPhF_3^-$ group, based on the following empirical data, $\sigma_R{}^\circ = 0.05(\delta(C_{para}) - \delta(C_{meta}))$ and $\sigma_I = 0.424(\delta(C_{meta}) - \delta(C_{benzene})) + 0.032(\delta(C_{para}) - \delta(C_{benzene}))$; Voronkov, M. G.; Glukhikh, V. I.; D'yakov, V. M.; Keiko, V. V.; Kuznetsova, G. A.; Yarosh, O. G. *Dokl. Akad. Nauk SSSR* **1981**, *258*, 387; *Dokl. Phys. Chem.* **1981**, *258*, 398. See also ref 1a. Somewhat different coefficients have also been reported.[13]

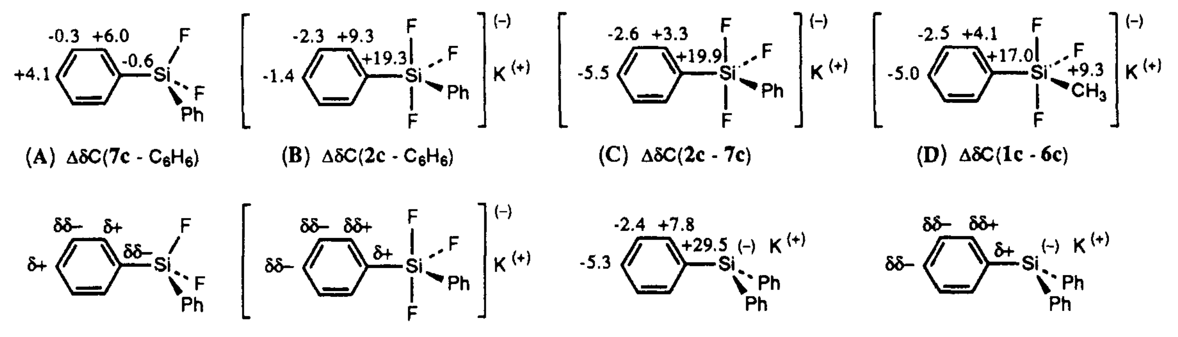

Figure 4. ^{13}C chemical shift changes on going from benzene to a tetracoordinate phenylsilane and pentacoordinate phenylsilicates, from phenylsilanes to phenylsilicates, and from benzene to a phenylsilyl anion (ref 19a) and charge distributions.

Table VIII. Changes in ^{13}C Chemical Shifts of Anionic pentacoordinate Silicates 1 and 2 vs Neutral Tetracoordinate Silanes 6 and 7, Respectively

	Δδ(C(silicate − silane))				
silicate − silane	C4	C3	C2	C1	$SiCH_3$
1a–6a (CF_3)	−5.41	−2.68	+3.10	+18.20	+8.98
1b–6b (Cl)	−5.50	−3.02	+4.26	+17.19	+9.24
1c–6c (H)	−4.96	−2.48	+4.05	+16.97	+9.34
1d–6d (Me)	−6.26	−2.37	+4.39	+16.55	+9.39
1e–6e (OMe)	−3.88	−2.97	+4.20	+16.37	+9.38
2a–7a (CF_3)	−5.92	−2.79	+2.58	+19.14	*a*
2b–7b (Cl)	−5.84	−2.76	+3.44	+20.15	*a*
2c–7c (H)	−5.53	−2.56	+3.30	+19.91	*a*
2d–7d (Me)	−6.97	−2.47	+3.70	+19.94	*a*
2e–7e (OMe)	−3.58	−2.71	+3.43	+20.11	*a*

[a] The corresponding data of the parent phenyl group are nearly constant as follows: C4′ −5.53 to −5.62; C3′ −2.56 to −2.66; C2′ +3.21 to +3.92; C1′ +19.91 to +20.41.

shown in **C** and **D**, respectively, in Figure 4. There are thus +17 to +20 ppm and +9.3 ppm downfield shifts for the Si ipso carbon (C1) of the phenyl group and for the saturated methyl carbon, respectively. The latter may be ascribed to the σ inductive effect and other possible effects such as steric effects.[16,17] With this value as the standard, the excess downfield shift, nearly +10 ppm, of the Si ipso carbon (C1) of the phenyl group may be ascribed primarily to the π inductive effect such as through-space π polarization (F_π) induced by the electric fields of charged substituents.[18] On the basis of the data in **C** and **D**, the charge distribution in the phenyl group is schematically represented as **B′**, being characteristic of the π polarization effect. The C1 atoms in **2c** and **1c** may thus become electron-deficient in comparison with those in **7c** and **6c**. This is a sharp contrast to the charge distribution **A′** in **7c**, where the resonance effect (R_π) is the predominant effect. It is worthy of note here that the electron distribution in the phenyl group in silicates is quite similar to that in silyl anions, which has also been explained by the electric field π polarization effect, as shown in **E** and **E′**.[19]

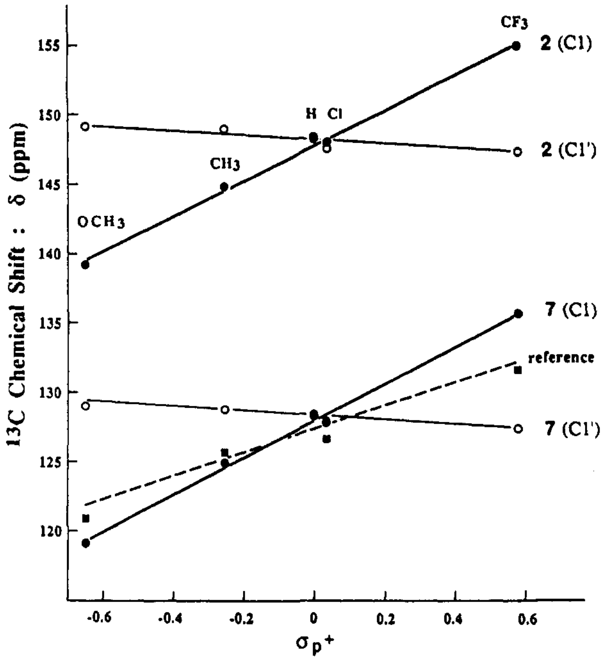

Figure 5. Hammett plots of ^{13}C chemical shifts of C1 (●) and C1′ (○) in **2** and **7**. Plot of para carbon chemical shifts in monosubstituted benzenes is shown for ref 14.

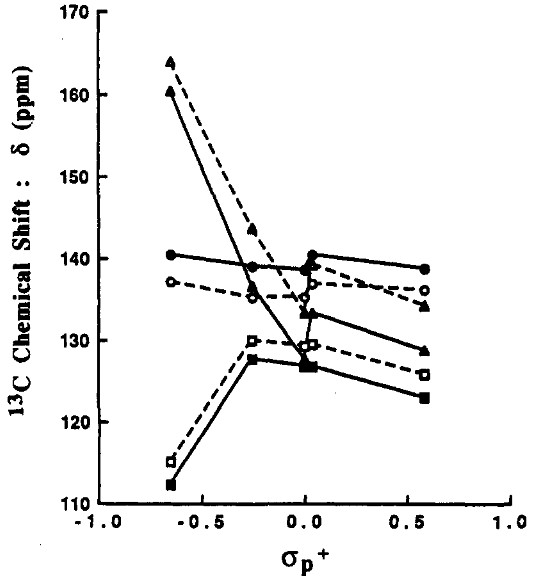

Figure 6. Hammett plots of ^{13}C chemical shifts of C2 (●), C3 (■), and C4 (▲) in **2** and C2 (○), C3 (□), and C4 (△) in **7**.

Finally, effects of para substituents are considered. Changes in ^{13}C chemical shifts for a series of para-substituted phenylsilicates from the corresponding silanes, Δδ(C(1 − 6)) and Δδ(C(2 − 7)), are summarized in Table VIII. The data clearly indicate that the changes in the

---

[16] Breitmaier, E.; Voelter, W. *Carbon-13 NMR Spectroscopy*; VCH: Weinheim, 1987; Chapter 3.

[17] The downfield shift, however, does not necessarily mean the electron deficiency of the methyl carbon. Theoretical studies on pentacoordinate silicates have shown an increase in electron densities on all ligand atoms in comparison with the corresponding tetracoordinate silanes.[3]

[18] (a) Reynolds, W. F. *Prog. Phys. Org. Chem.* **1983**, *14*, 165. (b) Katritzky, R. R.; Topsom, R. D. *J. Chem. Educ.* **1971**, *48*, 427.

[19] (a) Buncel, E.; Venkatachalan, T. K.; Eliasson, B.; Edlund, U. *J. Am. Chem. Soc.* **1985**, *107*, 303. (b) Olah, G. A.; Hunadi, R. *J. Am. Chem. Soc.* **1980**, *102*, 6989.

charge distribution during the structural change from neutral tetracoordinate silane to anionic pentacoordinate silicate are hardly influenced by the para substituents. Thus, the charge distribution in each case is essentially the same as that in the parent phenyl cases discussed above, suggesting the predominance of the π polarization effect in silicates.

(2) Electronic effects on the charge densities at the Si ipso (C1) carbons are estimated here. The ^{13}C chemical shifts of C1 (para to X) of the substituted phenyl group and C1′ of the parent phenyl group in silicates **2** and silanes **7** are plotted against Hammett σ^+ constants[9] of the substituents to give linear relationships, as shown in Figure 5,[13,14] while no linear relationships are obtained with other aromatic carbons, as shown in Figure 6;[20] however, all lines for silicate **2** are parallel to the respective lines for silane **7**. The parallelism reveals that *the mechanism of the transmission of the electronic effects by para substituents is little affected by structural change at silicon from tetracoordinate to pentacoordinate state.*

The linear relationships in Figure 5 are pertinent to the present discussion. As mentioned before, it has been established that there is a linear relationship between the chemical shift and the total charge densities, which is in turn correlated linearly with the Hammet σ_p^+, of the para carbons of monosubstituted benzenes.[13,14] Apparently, the rule can be applied to the present silyl-substituted cases. The parallel two lines, with about 20 ppm difference, for C1 (para to X) in **2** and **7** (r = 0.997 and 0.998) have positive signs, indicative of lower field shifts with electron-withdrawing substituents. Interestingly, the slopes are slightly larger than that of the reference line[14] for para carbons of monosubstituted benzenes, demonstrating that the Si ipso C1 (para to X) atoms in para substituted phenyl–silicon compounds are slightly more sensitive to the electronic effect by the para substituents than the para carbons in monosubstituted benzenes.

The linear relationships of C1′ of the parent phenyl groups in **2** and **7** are also interesting; the slopes are small negative, being opposite to the lines for C1. The silicon moieties seem to be almost an insulator for the transmission of the electronic effect between two ligands but definitely to reverse the electronic nature of C1′ vs C1. It may also be noted in this connection that tetracoordinate silicon and pentacoordinate silicon moieties behave similarly in the electronic effect transmission.

Difference in electron densities on the two Si ipso carbons C1 and C1′ may, therefore, be estimated from the chemical shift difference $\Delta\delta(C) = \delta(C1) - \delta(C1')$ between the two aromatic rings *in the same molecule*. If the empirical factor 450 ppm/e is employed,[13] $\Delta\delta(C) = +7.39$ ppm for **2a** (X = CF_3), +0.48 ppm for **2b** (X = Cl), −0.97 ppm for **2d** (X = Me), and −4.14 ppm for **2e** (X = OMe) correspond to +0.016 e, +0.001 e, −0.009 e, and −0.022 e differences, respectively (the positive sign means that C1 is more electron-deficient than C1′). Obviously, these electronic biases also apply roughly to the silanes.

The present aspects concerning the electronic effects observed in anionic pentacoordinate organosilicon species, especially the estimation of the charge density differences on the Si ipso carbons, should be useful for elucidation of reaction mechanisms of the silicon–carbon bond cleavage reactions which involve penta- and/or hexacoordinate anionic silicon species as key intermediates. We will discuss these aspects in the mechanistic study on the hydrogen peroxide oxidation of the silicon–carbon bond.[21]

Experimental Section

General Remarks. ^1H (200 MHz), ^{13}C (50.29 MHz), ^{19}F (188.15 MHz), and ^{29}Si (39.73 MHz) NMR spectra were recorded on a Varian VXR-200 spectrometer equipped with a VX-4000 computer. ^1H and ^{13}C chemical shifts were referenced to internal acetone-d_6 (^1H δ 2.05 ppm; ^{13}C δ 29.8 ppm) or $CDCl_3$ (^1H δ 7.24 ppm) relative to Me_4Si at δ 0.00 ppm. ^{19}F chemical shifts referred to $CFCl_3$ (^{19}F δ 0.00 ppm) as an internal standard. ^{29}Si chemical shifts were relative to Me_4Si in ppm. ^{29}Si NMR experiments were performed with proton decoupling, using a standard ^{13}C pulse program. Temperature calibration was accomplished by using a standard methanol sample, with a calibration error of ±1.0 °C.

Ether was distilled under N_2 from sodium/benzophenone, while benzene, tetrahydrofuran (THF), and toluene were distilled from lithium aluminum hydride.

Preparation of Diorganodichlorosilanes and Diorganodifluorosilanes. Arylmethyldichlorosilanes and unsymmetrical diaryldichlorosilanes were prepared in the usual manner from $MeSiCl_3$ and $PhSiCl_3$, respectively, by treatment with the appropriate arylmagnesium bromide in dry ether or dry ether–benzene, except some ortho-substituted diaryldichlorosilanes, as described below. Conversion of the dichlorosilanes into the corresponding difluorosilanes was carried out by treatment with an excess amount of antimony trifluoride at −50 °C to room temperature for 6–12 h, followed by filtration and distillation. Only one example is described herein. Yields, boiling points, spectral and high-resolution mass data for other chlorosilanes and difluorosilanes (**6** and **7**) are given in the supplementary material.

(1) 3,5-Xylyltrichlorosilane. A solution of 3,5-xylylmagnesium bromide was prepared from 3,5-xylyl bromide (25 g, 135 mmol) and magnesium (3.6 g, 149 mmol) in dry ether (100 mL). This Grignard solution was slowly added to a solution of silicon tetrachloride (18 mL, 157 mmol) in dry ether (100 mL) at 0 °C over 1 h under nitrogen, and the mixture was stirred at room temperature overnight. After filtration through Celite, the filtrate was evaporated and distilled to give 12.52 g (39%, based on the xylyl bromide) of 3,5-xylyltrichlorosilane: bp 117–120 °C (19 mmHg); ^1H NMR ($CDCl_3$, 200 MHz) δ 2.378 (s, 6 H), 7.209 (bs, 3 H), 7.401 (bs, 6 H); IR (liquid film, cm^{-1}) 2928 (s), 1602 (s), 1410 (s), 1276 (s), 1140 (vs), 870 (s), 850 (s), 690 (s); MS m/z (assignment, relative intensity) 242 ($M^+ + 4$, 8), 241 ($M^+ + 3$, 3), 240 ($M^+ + 2$, 20), 239 ($M^+ + 1$, 3), 105 (100).

(2) (2,6-Xylyl)(3,5-xylyl)dichlorosilane. To a solution of 2,6-xylyl bromide (6.03 mL, 45 mmol) in dry ether (90 mL) was added dropwise n-butyllithium (1.6 M in hexane, 50 mL, 80 mmol) at 0 °C over 10 min, and the mixture was stirred at room temperature overnight. The resulting 2,6-xylyllithium solution was added dropwise to a solution of 3,5-xylyltrichlorosilane (11 g, 46 mmol), prepared above, in ether (80 mL) at 0 °C over 1 h. After stirring at room temperature for 12 h, filtration through Celite, evaporation of solvents, and distillation gave 12.17 g (87% yield based on xylyl bromide) of the dichlorosilane: bp 135–137 °C (0.2 mmHg); ^1H NMR ($CDCl_3$) δ 2.339 (s, 6 H), 2.431 (s, 6 H), 7.037 (AB_2, J = 7.8 Hz, 2 H), 7.133 (bs, 1 H), 7.277 (AB_2, J = 7.8 Hz, 1 H), 7.375 (bs, 2 H); IR (liquid film, cm^{-1}) 2972 (s), 2932 (s), 1452 (vs), 1402 (s), 1138 (s), 858 (s), 774 (s), 694 (s); MS m/z (assignment, relative intensity) 308 (M^+, 14), 202 (11), 106 (100).

(3) (2,6-Xylyl)(3,5-xylyl)difluorosilane, $(2,6\text{-}Me_2C_6H_3)(3,5\text{-}Me_2C_6H_3)SiF_2$: 56% yield; bp 104–106 °C (0.15 mmHg); ^1H NMR (acetone-d_6) δ 2.302 (s, 6 H), 2.461 (t, J = 2.5 Hz, 6 H), 7.134 (AB_2, J = 7.4 Hz, 2 H), 7.237 (s, 1 H), 7.268 (s, 2 H), 7.367 (AB_2, J = 7.4 Hz, 1 H); ^{13}C NMR (acetone-d_6) δ 21.19, 23.56 (t, J = 3.0 Hz), 126.68 (t, $^2J_{CF}$ = 15.65 Hz), 129.01, 130.83 (t, $^2J_{CF}$ = 19.53 Hz), 131.94, 132.86, 134.60, 138.96, 146.04; ^{19}F NMR (acetone-d_6) δ − 131.04 ($^1J_{FSi}$ = 292.8 Hz); IR (liquid film, cm^{-1}) 1454 (s), 1146 (s), 888 (s), 834 (s), 776 (s), 696 (s), 600 (s); MS m/z (assignment, relative intensity) 277 ($M^+ + 1$, 24), 276 (M^+, 100), 261 (55), 106 (72), 104 (20); HRMS calcd for $C_{16}H_{18}F_2Si$ 276.1147, found 276.1169.

Preparation of the 18-Crown-6 Potassium Salt of Diorganotrifluorosilicate, $[RR'SiF_3^-][K^+\cdot 18\text{-crown-}6]$ (1 and 2). According to Damrauer's procedure,[4b] diorganodifluorosilane (**6** or **7**) (6 mmol) was stirred with spray-dried KF (5.5 mmol) and

---

(20) Essentially the same shapes have been obtained in plots of the aromatic carbon chemical shifts of **1** and **6**.

(21) Tamao, K.; Hayashi, T.; Ito, Y. Manuscript under preparation.

18-crown-6 (5 mmol) in toluene (10 mL) at room temperature for 1–2 days. The resulting white crystalline solids were collected by filtration. Recrystallization from THF gave pure silicate.

[(4-CF$_3$C$_6$H$_4$)MeSiF$_3^-$][K$^+$·18-crown-6] (1a): 32% yield; ^{1}H NMR (acetone-d_6, +22 °C) δ 0.080 (b, 3 H), 3.607 (s, 24 H), 7.454 (AB q, J = 7.40 Hz, 2 H), 8.069 (AB q, J = 7.40 Hz, 2 H); ^{13}C NMR (acetone-d_6, +22 °C) δ 3.65 (b), 70.66, 123.07 (q, $^3J_{\mathrm{CF}}$ = 1.23 Hz), 126.02 (q, $^1J_{\mathrm{CF}}$ = 269.22 Hz), 128.78 (q, $^2J_{\mathrm{CF}}$ = 30.98 Hz), 137.96, 155.09 (b); ^{19}F NMR (acetone-d_6, +22 °C) δ –61.60 (s, 3 F), –109.79 (b, 3 F); ^{19}F NMR (acetone-d_6, –78 °C) δ –60.20 (s, 3 F), –81.56 (q, $^3J_{\mathrm{FH}}$ = 8.84 Hz, $^1J_{\mathrm{FSi}}$ = 251.74 Hz, 2 F), –132.76 (s, $^1J_{\mathrm{FSi}}$ = 210.64 Hz, 1 F); IR (KBr, cm^{-1}) 1354 (s), 1330 (s), 1164 (s), 1112 (vs), 1058 (s), 966 (s), 808 (s), 752 (s), 668 (s). Anal. Calcd for C$_{20}$H$_{31}$F$_6$O$_6$SiK: C, 43.79; H, 5.70. Found: C, 43.50; H, 5.69.

[(4-ClC$_6$H$_4$)MeSiF$_3^-$][K$^+$·18-crown-6] (1b): 70% yield; mp 148.5–149.5 °C; ^{1}H NMR (acetone-d_6, +22 °C) δ 0.032 (b, 3 H), 3.631 (s, 24 H), 7.138 (AB q, J = 8.40 Hz, 2 H), 7.911 (AB q, J = 8.40 Hz, 2 H); ^{1}H NMR (acetone-d_6, –78 °C) δ –0.015 (t, $^3J_{\mathrm{HF}}$ = 19.20 Hz, 3 H), 3.541 (s, 24 H), 7.238 (AB q, J = 8.20 Hz, 2 H), 7.918 (AB q, J = 8.20 Hz, 2 H); ^{13}C NMR (acetone-d_6, +22 °C) δ 4.22 (br), 70.76, 126.67, 133.18, 139.99; ^{19}F NMR (acetone-d_6, +22 °C) δ –100.05 (b); ^{19}F NMR (acetone-d_6, –78 °C) δ –83.42 (q, $^3J_{\mathrm{FH}}$ = 8.28 Hz, $^1J_{\mathrm{FSi}}$ = 250.52 Hz, 2 F), –133.42 (s, $^1J_{\mathrm{FSi}}$ = 210.16 Hz, 1 F); IR (KBr, cm^{-1}) 2396 (vs), 1356 (s), 1252 (s), 1106 (vs), 966 (s), 804 (s), 762 (s), 664 (s). Anal. Calcd for C$_{19}$H$_{31}$ClF$_3$O$_6$SiK: C, 44.31; H, 6.07. Found: C, 44.02; H, 6.01.

[PhMeSiF$_3^-$][K$^+$·18-crown-6] (1c): 86% yield; mp 114.5–115 °C; ^{1}H NMR (acetone-d_6, +22 °C) δ 0.054 (b, 3 H), 3.620 (s, 24 H), 7.068–7.179 (m, 3 H), 7.887–7.984 (m, 2 H); ^{1}H NMR (acetone-d_6, –78 °C) δ 0.009 (t, $^3J_{\mathrm{HF}}$ = 9.80 Hz, 3 H), 3.536 (s, 24 H), 7.102–7.233 (m, 3 H), 7.879–7.999 (m, 2 H); ^{13}C NMR (acetone-d_6, + 22 °C) δ 70.82, 126.70, 127.38, 138.09; ^{19}F NMR (acetone-d_6, +22 °C) δ –99.68 (b); ^{19}F NMR (acetone-d_6, –78 °C) δ –83.85 (q, $^3J_{\mathrm{FH}}$ = 8.65 Hz, $^1J_{\mathrm{FSi}}$ = 251.37 Hz, 2 F), –133.22 (s, $^1J_{\mathrm{FSi}}$ = 210.16, 1 F); IR (KBr, cm^{-1}) 2904 (s), 1528 (vs), 1354 (s), 1250 (s), 1108 (vs), 968 (s). Anal. Calcd for C$_{19}$H$_{32}$F$_3$O$_6$SiK: C, 47.48; H, 6.71. Found: C, 47.10; H, 6.85.

[(4-MeC$_6$H$_4$)MeSiF$_3^-$][K$^+$·18-crown-6] (1d): 79% yield; mp 126–127 °C; ^{1}H NMR (acetone-d_6, +22 °C) δ 0.032 (b, 3 H), 2.231 (s, 3 H), 3.624 (s, 24 H), 6.946 (AB q, J = 7.70 Hz, 2 H), 7.833 (AB q, J = 7.70 Hz, 2 H); ^{1}H NMR (acetone-d_6, –78 °C) δ –0.012 (t, $^3J_{\mathrm{HF}}$ = 9.10 Hz, 3 H), 2.206 (s, 3 H), 3.546 (s, 24 H), 6.978 (AB q, J = 7.60 Hz, 2 H), 7.840 (AB q, J = 7.60 Hz, 2 H); ^{13}C NMR (acetone-d_6, +22 °C) δ 4.20 (b), 21.34, 70.68, 127.54, 136.40, 138.41; ^{19}F NMR (acetone-d_6, +22 °C) δ –99.63 (b); ^{19}F NMR (acetone-d_6, –78 °C) δ –84.37 (q, $^3J_{\mathrm{FH}}$ = 8.28 Hz, $^1J_{\mathrm{FSi}}$ = 248.92 Hz, 2 F), –133.24 (s, $^1J_{\mathrm{FSi}}$ = 210.35 Hz, 1 F); IR (KBr, cm^{-1}) 2904 (s), 1528 (vs), 1476 (s), 1354 (s), 1250 (s), 1108 (s), 968 (s). Anal. Calcd for C$_{29}$H$_{34}$F$_3$O$_6$SiK: C, 48.56; H, 6.93. Found: C, 48.31; H, 6.88.

[(4-MeOC$_6$H$_4$)MeSiF$_3^-$][K$^+$·18-crown-6] (1e): 27% yield; mp 122–122.5 °C; ^{1}H NMR (acetone-d_6, +22 °C) δ 0.028 (s, 3 H), 3.619 (s, 24 H), 3.728 (s, 3 H), 6.721 (AB q, J = 8.80 Hz, 2 H), 7.899 (AB q, J = 8.80, 2 H); ^{1}H NMR (acetone-d_6, –78 °C) δ –0.025 (t, $^3J_{\mathrm{HF}}$ = 8.60 Hz, 3 H), 3.547 (s, 24 H), 3.694 (s, 3 H), 6.745 (AB q, J = 8.30 Hz, 2 H), 7.901 (AB q, J = 8.30 Hz, 2 H); ^{13}C NMR (acetone-d_6, +22 °C) δ 4.20 (b), 54.92, 70.74, 112.36, 140.00, 160.14; ^{19}F NMR (acetone-d_6, +22 °C) δ –98.43 (b); ^{19}F NMR (acetone-d_6, –78 °C) δ –84.57 (q, $^3J_{\mathrm{FH}}$ = 7.71 Hz, $^1J_{\mathrm{FSi}}$ = 250.52 Hz, 2 F), –133.10 (s, $^1J_{\mathrm{FSi}}$ = 210.92 Hz, 1 F); IR (KBr, cm^{-1}) 2900 (vs), 1530 (vs), 1354 (s), 1254 (s), 1108 (vs), 968 (s), 806 (s), 662 (s). Anal. Calcd for C$_{20}$H$_{34}$F$_3$O$_7$SiK: C, 47.04; H, 6.71. Found: C, 46.92; H, 6.61.

[(4-CF$_3$C$_6$H$_4$)PhSiF$_3^-$][K$^+$·18-crown-6] (2a): 58% yield; mp 182.5–183.0 °C; ^{1}H NMR (acetone-d_6) δ 3.634 (s, 24 H), 7.098–7.190 (m, 3 H), 7.397–7.493 (m, 2 H), 7.977–8.080 (m, 2 H), 8.106–8.208 (m, 2 H); ^{19}F NMR (acetone-d_6, +22 °C) δ –61.70 (s, 3 F), –109.90 (b, 3 F); ^{19}F NMR (THF-d_8, –90 °C) –59.69 (s, 3 F), –101.02 ($^1J_{\mathrm{FSi}}$ = 253.81 Hz, 2 F), –134.33 ($^1J_{\mathrm{FSi}}$ = 206.40 Hz, 1 F); ^{29}Si NMR (acetone-d_6) δ –110.44 ($^1J_{\mathrm{SiF}}$ = 239.73 Hz); IR (KBr, cm^{-1}) 1356 (s), 1326 (s), 1162 (s), 1104 (vs), 1058 (s), 964 (s), 548 (s). Anal. Calcd for C$_{25}$H$_{33}$F$_6$O$_6$SiK: C, 49.17; H, 5.45. Found: C, 48.99; H, 5.55.

[(4-ClC$_6$H$_4$)PhSiF$_3^-$][K$^+$·18-crown-6] (2b): 43% yield; mp 163–164 °C; ^{1}H NMR (acetone-d_6) δ 3.600 (s, 24 H), 7.105–7.217 (m, 5 H), 7.946–8.073 (m, 4 H); ^{19}F NMR (acetone-d_6, +22 °C) δ –110.27 (b); ^{19}F NMR (THF-d_8, –90 °C) δ –101.79 ($^1J_{\mathrm{FSi}}$ = 253.81 Hz, 2 F), –134.19 ($^1J_{\mathrm{FSi}}$ = 206.97 Hz, 1 F); IR (KBr, cm^{-1}) 1108 (vs), 966 (s). Anal. Calcd for C$_{24}$H$_{33}$ClF$_3$O$_6$SiK: C, 49.95; H, 5.76. Found: C, 50.06; H, 5.69.

[Ph$_2$SiF$_3^-$][K$^+$·18-crown-6] (2c): 41% yield; mp 122.5–123.0 °C; ^{1}H NMR (acetone-d_6) δ 3.552 (s, 24 H), 7.114–7.215 (m, 3 H), 8.008–8.092 (m, 2 H); ^{19}F NMR (acetone-d_6, –85 °C) δ –99.55 ($^1J_{\mathrm{FSi}}$ = 255.13 Hz, 2 F), –132.69 ($^1J_{\mathrm{FSi}}$ = 205.65 Hz); ^{29}Si NMR (acetone-d_6) δ –109.06 ($^1J_{\mathrm{SiF}}$ = 238.06 Hz); IR (KBr, cm^{-1}) 2900 (s), 1354 (s), 1108 (vs), 964 (s), 788 (s), 742 (s), 716 (s), 704 (s), 668 (s). Anal. Calcd for C$_{24}$H$_{34}$O$_6$F$_3$SiK: C, 53.03; H, 6.35. Found: C, 53.12; H, 6.31.

[(4-MeC$_6$H$_4$)PhSiF$_3^-$][K$^+$·18-crown-6] (2d): 54% yield; mp 127–128 °C; ^{1}H NMR (acetone-d_6) δ 2.252 (s, 3 H), 3.595 (s, 24 H), 7.013 (AB q, J = 7.9 Hz, 2 H), 7.114–7.221 (m, 3 H), 7.861–8.040 (m, 2 H), 7.910 (AB q, J = 7.9 Hz, 2 H); ^{19}F NMR (acetone-d_6, +22 °C) δ –110.78 (b); ^{1}H NMR (acetone-d_6, –78 °C) δ –99.99 ($^1J_{\mathrm{FSi}}$ = 251.56 Hz, 2 F), –133.04 ($^1J_{\mathrm{FSi}}$ = 206.02 Hz, 1 F); ^{29}Si NMR (acetone-d_6) δ –109.71 ($^1J_{\mathrm{SiF}}$ = 237.74 Hz); IR (KBr, cm^{-1}) 1354 (s), 1106 (vs), 966 (s), 752 (s), 692 (s). Anal. Calcd for C$_{25}$H$_{36}$O$_6$F$_3$SiK: C, 53.94; H, 6.52. Found: C, 54.08; H, 6.49.

[(4-MeOC$_6$H$_4$)PhSiF$_3^-$][K$^+$·18-crown-6] (2e): 62% yield; mp 155–156 °C; ^{1}H NMR (acetone-d_6) δ 3.596 (s, 24 H), 3.725 (s, 3 H), 6.737 (AB q, J = 8.8 Hz, 2 H), 7.073–7.162 (m, 3 H), 7.957–8.062 (m, 2 H), 8.008 (AB q, J = 8.8 Hz, 2 H); ^{19}F NMR (acetone-d_6, +22 °C) δ –109.70 (b), ^{19}F NMR (THF-d_8, –90 °C) δ –102.53 ($^1J_{\mathrm{FSi}}$ = 249.11 Hz, 2 F), –133.69 ($^1J_{\mathrm{FSi}}$ = 203.96 Hz, 1 F); ^{29}Si NMR (acetone-d_6) δ –110.04 ($^1J_{\mathrm{SiF}}$ = 237.82 Hz); IR (KBr, cm^{-1}) 1108 (vs), 966 (s). Anal. Calcd for C$_{25}$H$_{36}$O$_7$F$_3$SiK: C, 52.43; H, 6.34. Found: C, 52.30; H, 6.37.

[(4-Me$_2$NC$_6$H$_4$)PhSiF$_3^-$][K$^+$·18-crown-6] (2f): 39% yield; mp 166–167 °C; ^{1}H NMR (acetone-d_6) δ 2.853 (s, 6 H), 3.622 (s, 24 H), 6.598 (AB q, J = 8.8 Hz, 2 H), 7.035–7.134 (m, 3 H), 7.901–8.026 (m, 2 H), 7.952 (AB q, J = 8.8 Hz, 2 H); ^{13}C NMR (acetone-d_6, +45 °C) δ 40.70, 70.84, 112.11, 126.80, 127.49, 138.08, 140.16, 151.57; IR (KBr, cm^{-1}) 1106 (vs), 688 (s). Anal. Calcd for C$_{26}$H$_{39}$F$_3$O$_6$F$_3$NSiK: C, 53.31; H, 6.71. Found: C, 53.11; H, 6.85.

[(2-MeC$_6$H$_4$)PhSiF$_3^-$][K$^+$·18-crown-6] (3a): 43% yield; mp 122.5–123.5 °C; ^{1}H NMR (acetone-d_6) δ 2.467 (s, 3 H), 3.534 (s, 24 H), 6.934–6.995 (m, 3 H), 7.168–7.263 (m, 3 H), 7.423–7.523 (m, 1 H), 8.059–8.163 (m, 2 H); ^{19}F NMR (acetone-d_6, +22 °C) δ –103.09 (b); ^{19}F NMR (acetone-d_6, –90 °C) δ –89.18 ($^1J_{\mathrm{FSi}}$ = 253.82 Hz, 2 F), –131.03 ($^1J_{\mathrm{FSi}}$ = 211.29 Hz, 1 F); IR (KBr, cm^{-1}) 2896 (s), 1354 (s), 1110 (vs), 968 (s), 704 (s), 672 (s). Anal. Calcd for C$_{25}$H$_{36}$F$_3$O$_6$SiK: C, 53.94; H, 6.52. Found: C, 53.71; H, 6.51.

[(3-MeC$_6$H$_4$)PhSiF$_3^-$][K$^+$·18-crown-6] (3b): 50% yield; mp 140–141 °C; ^{1}H NMR (acetone-d_6) δ 2.267 (s, 3 H), 3.557 (s, 24 H), 6.927–7.113 (m, 2 H), 7.116–7.212 (m, 3 H), 7.780–7.896 (m, 2 H), 7.978–8.096 (m, 2 H); ^{19}F NMR (acetone-d_6, +22 °C) δ –109.79 (b); ^{19}F NMR (acetone-d_6, –90 °C) δ –99.39 ($^1J_{\mathrm{FSi}}$ = 239.33 Hz, 2 F), –132.85 ($^1J_{\mathrm{FSi}}$ = 208.66 Hz, 1 F); IR (KBr, cm^{-1}) 1110 (s). Anal. Calcd for C$_{25}$H$_{36}$O$_6$F$_3$SiK: C, 53.94; H, 6.52. Found: C, 53.72; H, 6.46.

[(2,6-Me$_2$C$_6$H$_3$)PhSiF$_3^-$][K$^+$·18-crown-6] (3c): 75% yield; mp 142.0–142.5 °C; ^{1}H NMR (acetone-d_6) δ 2.392 (s, 6 H), 3.525 (s, 24 H), 6.746 (A of A$_2$B, J_{AB} = 7.8 Hz, 2 H), 6.837 (B of A$_2$B, J_{AB} = 7.8 Hz, 1 H) 7.166–7.257 (m, 3 H), 8.060–8.174 (m, 2 H); ^{19}F NMR (acetone-d_6, +22 °C) δ –91.81 (b); ^{19}F NMR (acetone-d_6, –90 °C) δ –88.74 ($^1J_{\mathrm{FSi}}$ = 255.14 Hz, 2 F), –126.97 ($^1J_{\mathrm{FSi}}$ = 214.31 Hz, 1 F); IR (KBr, cm^{-1}) 2908 (vs), 1353 (s), 1112 (vs), 968 (s), 746 (s), 678 (s), 586 (s), 512 (s). Anal. Calcd for C$_{26}$H$_{38}$O$_6$F$_3$SiK: C, 54.71; H, 6.71. Found: C, 54.51; H, 6.85.

[(3,5-Me$_2$C$_6$H$_3$)PhSiF$_3^-$][K$^+$·18-crown-6] (3d): 84% yield; mp 151–152 °C; ^{1}H NMR (acetone-d_6) δ 2.230 (s, 6 H), 3.561 (s, 24 H), 6.796 (s, 1 H), 7.100–7.202 (m, 3 H), 7.645 (s, 2 H), 7.976–8.083 (m, 2 H); ^{19}F NMR (acetone-d_6, +22 °C) δ –108.92 (b); ^{19}F NMR (acetone-d_6, –90 °C) δ –99.01 ($^1J_{\mathrm{FSi}}$ = 244.22 Hz, 2 F), –132.82 ($^1J_{\mathrm{FSi}}$ = 207.34 Hz, 1 F); IR (KBr, cm^{-1}) 1110 (s), 686 (s). Anal. Calcd for C$_{26}$H$_{38}$O$_6$F$_3$SiK: C, 54.71; H, 6.71. Found: C, 54.70; H, 6.86.

[(2,4,6-Me$_3$C$_6$H$_2$)PhSiF$_3^-$][K$^+$·18-crown-6] (3e): 57% yield; mp 133.5–134.5 °C; ^{1}H NMR (acetone-d_6) δ 2.149 (s, 3 H), 2.357 (s, 6 H), 3.521 (s, 24 H), 6.580 (s, 2 H), 7.135–7.252 (m, 3 H), 8.053–8.170 (m, 2 H); ^{19}F NMR (acetone-d_6, +22 °C) δ –92.70 (b); ^{19}F NMR (acetone-d_6, –90 °C) δ –88.43 ($^1J_{\mathrm{CF}}$ = 253.82 Hz, 2 F), –126.96 ($^1J_{\mathrm{CF}}$ = 213.74 Hz, 1 F); IR (KBr, cm^{-1}) 2896 (bs), 1354 (s), 1110 (bs), 966 (s), 502 (s). Anal. Calcd for C$_{27}$H$_{40}$O$_6$F$_3$SiK:

C, 55.46; H, 6.89. Found: C, 55.22; H, 7.11.

[(2-MeC_6H_4)(4-MeC_6H_4)SiF_3^-][K^+·18-crown-6] (4): 61% yield; mp 125–126 °C; ^1H NMR (acetone-d_6) δ 2.302 (s, 3 H), 2.467 (s, 3 H), 6.846–6.995 (m, 3 H), 7.058 (AB q, J = 8.0 Hz, 2 H), 7.426–7.514 (m, 1 H), 8.022 (AB q, J = 8.0 Hz, 2 H); ^{19}F NMR (acetone-d_6, +22 °C) δ −103.23 (b); ^{19}F NMR (acetone-d_6, −90 °C) δ −89.29 ($^1J_{FSi}$ = 227.10 Hz, 2 F), −130.86 ($^1J_{CF}$ = 208.47 Hz, 1 F); IR (KBr, cm^{-1}) 1110 (vs). Anal. Calcd for $C_{26}H_{38}O_6F_3SiK$: C, 54.71; H, 6.71. Found: C, 54.42; H, 6.77.

[(2,6-$Me_2C_6H_3$)(3,5-$Me_2C_6H_3$)SiF_3^-][K^+·18-crown-6] (5): 41% yield; mp 124.5–125.0 °C; ^1H NMR (acetone-d_6) δ 2.259 (s, 6 H), 2.392 (s, 6 H), 3.533 (s, 24 H), 6.736 (AB_2, J = 8.2 Hz, 2 H), 6.826 (AB_2, J = 8.2 Hz, 1 H), 6.837 (s, 1 H), 7.719 (s, 2 H); ^{19}F NMR (acetone-d_6, +22 °C) δ −90.03 (b); ^{19}F NMR (acetone-d_6, −90 °C) δ −87.96 ($^1J_{FSi}$ = 258.71 Hz), −126.65 ($^1J_{FSi}$ = 214.31 Hz); IR (KBr, cm^{-1}) 1108 (vs). Anal. Calcd for $C_{28}H_{42}O_6F_3SiK$: C, 56.16; H, 7.07. Found: C, 55.95; H, 7.13.

Variable-Temperature ^{19}F NMR Studies. The variable-temperature ^{19}F NMR studies have been carried out in a THF-d_8 solution of silicates (30–50 mg). The energy barriers for intramolecular ligand exchange ($\Delta G^{\ddagger}$, kcal/mol) were calculated by the Eyring equation.

X-ray Studies. Intensity data were collected on a Rigaku AFC-5R diffractometer using graphite-monochromatized Cu Kα radiation (λ = 1.541 78 Å) and ω–2θ scan values of 20 reflections in the range 35° ≤ 2θ ≤ 40°. No significant changes in intensities of three standard reflections monitored every 100 measurements were observed during data collection. The structures were solved by use of the program MULTAN87[22] and refined by the block-diagonal least-squares method to minimize the function of $\sum(w|\Delta F|^2)$. Corrections for absorption were applied after isotropic least-squares refinement for the non-H atoms, by an empirical method based on the differences between the observed and calculated structure factors.[23] Many of the H atoms were located in a difference electron density map, the others being stereochemically positioned. Positional parameters of all the atoms and anisotropic thermal ones of the non-H atoms were refined: the temperature factor of each H atom was assumed to be isotropic and estimated to be equal to the equivalent isotropic temperature factor of the bonded atom. Atomic scattering factors were calculated by the analytical appoximation, $\sum[a_i \exp(-b_i (\sin^2 \theta)\lambda^{-2})] + c$ (i = 1, ..., 4).[24] All computations were performed on a FACOM M-340R computer at Shionogi Research Laboratories. Crystallographic details are listed in Table II. Bond lengths for 18-crown-6 parts of all the compounds, in which the atoms are subjected to thermal motions of a large anisotropy, are shorter than the corresponding normal values.

The crystals of **2a**, **2e**, and **4** used for the X-ray study were recrystallized from THF, while those of **2d**, **2f**, and **5**, from acetone. For **2a**, the trifluoromethyl group is disordered, with an equal probability, at the two locations related approximately by a 2-fold axis imagined to lie along the C4–C13 direction. In Figure 1, one of the locations is shown for clarity. For **4**, the relatively large R value was attained due to poor quality of the crystal (chimneylike crystal) and large thermal motions exhibited especially in the 18-crown-6 part. Therefore, the geometrical data are inadequate to compare with those of other compounds.

Acknowledgment. We thank Professor Isao Morishima of the Division of Molecular Engineering, Graduate School of Engineering, Kyoto University, for valuable discussion concerning the ^{13}C NMR spectra. Thanks are also due to the Ministry of Education, Science, and Culture, Japan, for the Grant-in-Aid for Scientific Research on Priority Area of Organic Unusual Valency (No. 02247103).

Registry No. **1a**, 137364-49-9; **1b**, 137364-51-3; **1c**, 102307-93-7; **1d**, 137364-53-5; **1e**, 137364-55-7; **2a**, 137364-57-9; **2b**, 137364-59-1; **2c**, 102307-90-4; **2d**, 137364-61-5; **2e**, 137364-63-7; **2f**, 137364-65-9; **3a**, 137364-67-1; **3b**, 137364-69-3; **3c**, 119818-70-1; **3d**, 137393-38-5; **3e**, 137364-71-7; **4**, 137364-73-9; **5**, 137364-75-1; **6a**, 137364-33-1; **6b**, 137364-34-2; **6c**, 328-57-4; **6d**, 51501-86-1; **6e**, 137364-35-3; **7a**, 137364-37-5; **7b**, 137364-38-6; **7c**, 312-40-3; **7d**, 20988-21-0; **7e**, 137364-39-7; **7f**, 137364-40-0; (4-$CF_3C_6H_4$)MeSiCl_2, 339-57-1; (4-$Cl_3C_6H_4$)MeSiCl_2, 825-93-4; (4-MeC_6H_4)MeSiCl_2, 18236-57-2; (4-MeOC_6H_4)MeSiCl_2, 18236-55-0; (2-MeC_6H_4)MeSiCl_2, 18236-56-1; (4-$CF_3C_6H_4$)PhSiCl_2, 137364-26-2; (4-ClC_6H_4)PhSiCl_2, 834-68-4; (4-MeC_6H_4)PhSiCl_2, 13788-41-5; (4-MeOC_6H_4)PhSiCl_2, 137364-27-3; (4-$Me_2NC_6H_4$)PhSiCl_2, 137364-28-4; (2-MeC_6H_4)PhSiCl_2, 38948-60-6; (3-MeC_6H_4)PhSiCl_2, 13688-71-6; (3,5-$Me_2C_6H_3$)PhSiCl_2, 137364-29-5; (2-MeC_6H_4)(4-MeC_6H_4)SiCl_2, 137364-30-8; (2,6-$Me_2C_6H_3$)PhSiCl_2, 137364-31-9; (2,4,6-$Me_3C_6H_2$)PhSiCl_2, 137364-32-0; (2-MeC_6H_4)MeSiF_2, 137364-36-4; (2-MeC_6H_4)PhSiF_2, 137364-41-1; (3-MeC_6H_4)PhSiF_2, 137364-42-2; (2-MeC_6H_4)(4-MeC_6H_4)SiF_2, 137364-43-3; (2,6-$Me_2C_6H_3$)PhSiF_2, 119795-64-1; (3,5-$Me_2C_6H_3$)PhSiF_2, 137364-44-4; (2,4,6-$Me_3C_6H_2$)PhSiF_2, 137364-45-5; MeSiCl_3, 75-79-6; PhSiCl_3, 98-13-5; 3,5-xylyltrichlorosilane, 2942-84-9; 3,5-xylyl bromide, 556-96-7; silicon tetrachloride, 10026-04-7; (2,6-xylyl)(3,5-xylyl)dichlorosilane, 137364-46-6; 2,6-xylyl bromide, 19393-92-1; (2,6-$Me_2C_6H_3$)(3,5-$Me_2C_6H_3$)SiF_2, 137364-47-7.

Supplementary Material Available: Tables of atomic coordinates, thermal parameters, and bond lengths and angles for **2a**, **2d**, **2e**, **2f**, **4**, and **5** (Part 1, Tables S-I–S-XVIII) and a textual presentation of preparative methods and physical and spectral data of diorganodichlorosilanes and diorganodifluorosilanes including **6** and **7** (Part 2) (32 pages); listings of structure factors for **2a**, **2d**, **2e**, **2f**, **4**, and **5** (Tables S-XIX–S-XXIV) (152 pages). Ordering information is given on any current masthead page.

---

[22] Debaerdemaeker, T.; Germain, G.; Main, P.; Tate, C.; Woolfson, M. M. *MULTAN87 Computer Programs for the Automatic Solution of Crystal Structures form X-ray Diffraction Data*; University of York: York, England, 1987.

[23] Walker, N.; Staurt, D. *Acta Crystallogr.* **1983**, *A39*, 158.

[24] Cromer, D. T.; Waber, J. T. *International Tables for X-ray Crystallography*; Kynoch Press: Birmingham, England, 1973; Vol. IV, Table 2.2B.